Journal of the Optical Society of Korea, Vol. 8, No. 1, March 2004, pp. 6-12

Bragg Gratings Generated by Coupling of Surface Plasmons Induced on Metal Nanoparticles

Hyong Sik Won, Ki-young Choi, Seok Ho Song*, Cha-Hwan Oh, and Pill-Soo Kim

Microoptics National Research Laboratory (NRL), Department of Physics, Hanyang University, Seoul 133-791, KOREA

Dongwook Shin

Department of Ceramic Engeering, Hanyang University, Seoul 133-791, KOREA

(Received February 24, 2004)

Diffraction Bragg gratings consisting of metal (silver) nanoparticles are generated inside a soda-lime glass substrate. After ion-exchanging and annealing processes in the glass, the silver nanoparticles are first formed with the particle diameters of 10 nm ~ 30 nm. By interfering two CW laser beams at ~ 60 μm deep under the surface of the nanoparticles-dispersed glass, Bragg gratings with thickness of 15 μm and period of 3.5 μm are generated. Diffraction efficiency of the gratings formed by two TE-polarized beams is three times higher than that by two TM-polarized beams. From this polarization dependence, we have found that strong coupling of the surface plasmons induced on the metal particles may contribute dominantly to generate the diffraction grating.

OCIS codes : 240.5420, 050.1950

I. INTRODUCTION

One of the interesting characteristics of metallic nanoparticles is their exhibition of strong absorption peaks in the visible spectral range [1]. The peaks are mainly due to the resonantly excited particle plasmons of surface electromagnetic (EM) modes of the metal nanoparticles. Local field enhancement of the plasmons is influenced by the shape and size of the metal particles with typical size of less than 100 nm, as well as the material constants of the metal and the surrounding host medium. For a cluster of metallic nanoparticles, the field enhancement is additionally influenced by two types of plasmon interaction: dipolar far-field coupling and evanescent near-field coupling [2,3]. The far-field coupling causes conversion of the locally enhanced fields from evanescent to radiative in character via collective dipolar radiation from a particular periodic arrangement of the nanoparticles. Light transport via chains of metal particles [4], transmitting light through sub-wavelength hole arrays in a metal film [5], and beaming light with a single sub-wavelength aperture flanked by periodic surface corrugations [6] would be described by the far-field interaction of the resonant plasmons excited on every periodic of the indentations.

On the other hand, the near-field coupling within distance of the order of the particle diameter (~tens of nm), corresponding to the multipolar interactions between the particles, modifies the optical permittivity of the composite material embedding the metal particles. Abnormal dependence of the optical permittivity on density distribution of the metal particles dispersed in the metallic thin film can be also understood by this near-field coupling effect. Yano., et al [7] reported a good agreement in the effective permittivity, $\bar{\varepsilon}_m$, of thin metal films between experimental results and theoretical analysis based on the modified effective medium theory of $(\bar{\varepsilon}_m-1)/(\bar{\varepsilon}_m+2)=f(\varepsilon_m-1)/(\varepsilon_m+2)$, where f is a volume fraction of metal particles in the composite film, and ε_m is the permittivity of the bulk metal composing the metal particles. As the volume fraction goes up to one from zero, real and imaginary parts of the effective permittivity vary in the range of more than 19 enclosing zero permittivity. In particular, these values undergo sudden change around the critical film thickness ($f \sim 0.8$) which is possibly due to the strong near-field coupling of the particle plasmons. Therefore, use of composite media containing metallic nanoparticles may afford us another degree of freedom to choose dielectric materials for manipulating photonic band gap (PBG) structures [8,9], or even for realizing meta-materials with an extraordinary behavior, such as

negative refraction [10].

Periodic distribution of metallic nanoparticles in a dielectric medium can be accomplished by two-photon femtosecond laser-induced photoreduction of metal ions doped into the dielectric [11]. In the reference, they report that the laser-material interaction is initialized with a photochemical reaction, leading to particle precipitation and protrusion out of the flat sample surface. Distribution of the nanoparticles on the sample surface basically follows the light intensity distribution: larger volume fraction appears at the bright interference fringes, while at the dark region both the particle size and the volume fraction are small. In the photoreduction process, the plasmon coupling effect was not considered since the precipitated particles assumed to be far apart from each other. If the dielectric medium initially contains metal nanoparticles, instead of metal ions, and if the initial volume concentration of the particles inside the dielectric medium is large enough for near-field interacting, the periodic manipulation by the two-beam interferential fringes may be determined by a quite different mechanism. Irradiating this particle-dispersed sample with an intense, linearly polarized continuous-wave laser, the sample may be strongly influenced by the near-field coupling of the particle plasmons.

In this paper, we report the influence of the near-field coupling effect on periodic arrangement of the volume fraction of silver nanoparticles embedded in a glass medium. As an example of one-dimensional PBG structures, we present experimental results of diffraction Bragg gratings which are composed by silver nanoparticles dispersed periodically inside the medium. We have found that the near-field interaction between the particle plasmons excited by intense, linearly polarized, continuous-wave laser beams would not only accelerate deformation of the silver nanoparticles to exhibit dichroic axes being parallel to the polarization direction of the laser light [12], but also activate photochemical ionization (or, photoionization) of them. When the polarization direction of the two beams which interfere inside the glass medium is parallel to the planes of the interference fringes, the near-field coupling is enhanced so strongly enough that the silver particles at the bright interference fringes are ionized, diffused, and aggregated to the existing particles in the dark regions. In consequence, at the dark interference fringes possess a larger volume fraction due to increase of both the particle size and the number density, which would be reversed relative to the particle distribution generated by the femtosecond laser-induced photoreduction mentioned above. The two beams with the polarization direction being perpendicular to the fringe planes induce only a weak coupling between the particle plasmons which may not be enough to excite the photochemical ionization in the bright regions.

II. EXPERIMENTS AND RESULTS

The silver nanoparticles with diameters between 5 nm and 30 nm were prepared by double ion-exchanging between silver and sodium ions in a glass medium [13] and by annealing at temperature range of 500℃ ~700℃. At the first ion-exchange of silver for sodium ions, commercial soda-lime glass substrates with thickness of 1 mm were immersed for 5 hours in a molten-salt bath with 20% molar concentration of $AgNO_3$ in $NaNO_3$ at 360℃. At the second ion-exchange for 30 min in pure $NaNO_3$ molten at 360℃, only the silver ions near the glass surface were replaced again by the sodium ions while the rest of them, doped deeply inside the glass substrate, remained. The second ion-exchange was taken to avoid interaction between silver ion and air during laser irradiation and the deposition of a silver layer on the surface of the glass substrate by thermal diffusion of silver ions during the laser irradiation process. Fig. 1 shows metal gratings formed on glass after laser irradiation at only silver ion-exchanged glass. It shows gratings made by corrugated silver thin films on a glass surface which were generated by laser induced thermal diffusion of silver ions.

The silver ion-doped substrates were then annealed for 30 min in an air-conditioned electric furnace at the temperatures of 500, 550, 600, 650, and 700℃. The annealings caused a precipitation of metallic silver to form nm-size clusters inside the glass medium with a different volume fraction according to the annealing temperatures. It is noted that after the annealing there were no silver particles protruded out of the flat sample surface, and that the depth and thickness of the silver cluster layer under the glass surface were estimated to be about 60 μm and 15 μm, respectively, by measuring the interference pattern as will be described in accordance with Fig. 3. The formation of the silver cluster layer inside the glass substrate is evidenced by analyzing (a) the transmission electron microscope (TEM) image,

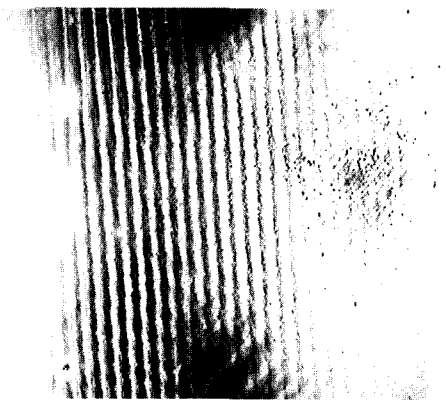

FIG. 1. Metallic gratings formed on the surface of the glass.

(b) the X-ray diffraction (XRD) spectra, and (c) the optical absorption spectra reported in Fig. 2. The electron transparent sample was prepared by mechanical grinding from the both sides of the glass substrate and by planar ion milling. Fig. 2 (a) shows a TEM image of the silver nanoclusters after annealing in air for 30 min at 600℃. Dark spots represent the silver nanoparticles with diameters of about 5-30 nm and spacing between the particles of about 20-50 nm. Increase in the volume fraction of the silver nanoparticles according to the annealing temperatures is observed by the XRD and absorption spectra shown in Fig. 2 (b) and Fig. 2 (c). For the sample annealed at 500℃, there are no diffraction peaks from the silver metal. This means that the annealing temperature is not enough to precipitate and form a metallic silver to be measurable. But, at 600 and 700℃ the intensity of the XRD peaks for |111⟩ and |200⟩ silver-crystal faces increases with the annealing temperature. This is due to increase of the volume fraction and the size of the silver particles. The particle size can be estimated from the Scherrer equation [14] by assuming that the clusters, of spheroidal shape, exhibit an uniform size. For an example, the particle diameter of the 700℃ annealed sample would be deduced as ~16 nm from the FWHM width of $2\Delta\theta \sim 0.3°$ for the |111⟩ peak in Fig. 2 (b), which is reasonably correlated with the TEM measurement. The absorption spectra shown in Fig. 2 (c) display an optical absorption band peaked at about 410 nm ~ 430 nm, typical of surface-plasmon-resonance absorption of the metallic silver nanoclusters having diameter of the order of 10 nm. The intensity of the absorption peak increases with the annealing temperature due to the increase of the volume fraction of silver particles. Particle size can be estimated from absorption spectrum by using the Mie scattering calculation. Figure 3 shows a comparison of absorption spectra experimentally measured and calculated by the Mie theory. In Fig. 3 the solid line is the absorption spectrum of the ion-exchanged glass annealed at 600℃ and the dash line is calculated. Size of the nanoparticle is 18 nm and the

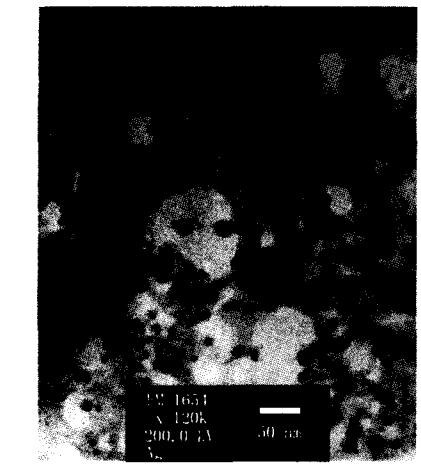

(a)

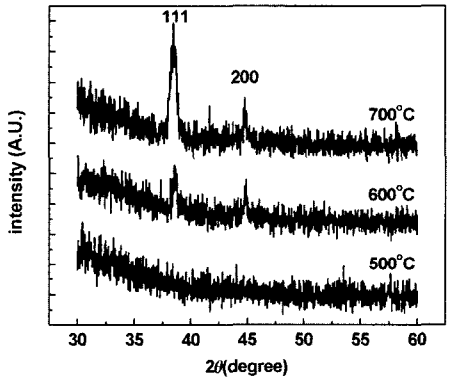

(b)

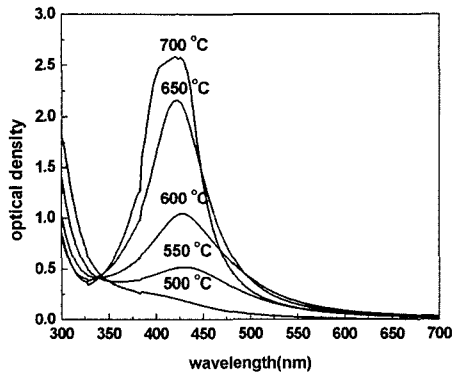

(c)

FIG. 2. (a) TEM image of silver nanoclusters, after annealing in air for 30 min at 600℃, (b) absorption spectra and (c) XRD spectra of the silver dispersed samples annealed for 30 min at different temperatures.

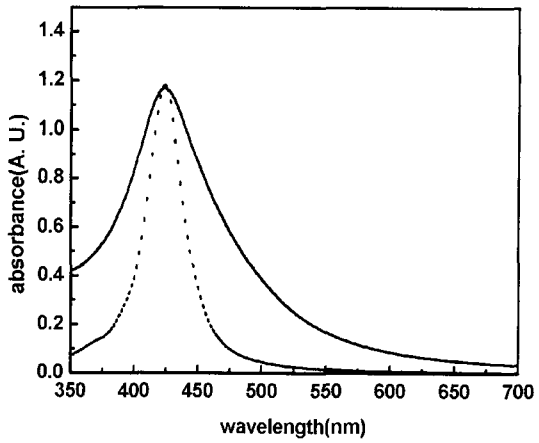

FIG. 3. Comparison between the experimental absorption spectrum and the theoretical one calculated by the Mie scattering theory.

refractive index of the surrounding medium is 1.5. Within these conditions, Fig. 3 shows a good agreement of the center wavelengths between the two absorption spectra. The particle size estimated by the Mie calculation is similar with that deduced from the XRD data and is reasonably correlated with the TEM measurement. A smaller band width of the calculated absorption spectrum than the experimental band width is due to the broad size-distribution of the sample used in the experiment.

In order to form an embedded Bragg grating by two-beam interference, we focused two linearly polarized beams, from a 700 mW, 488 nm, continuous-wave Ar-ion laser, on a same 200 μm-diameter spot at the silver-cluster-doped layer annealed at 600℃ for 30 min. The angle between the two incident beams was about 3 degrees, resulting in a two-beam interference pattern of 3.5-μm-period linear fringes at the focused plane. The beam intensity at the foci was about 10W/mm^2 and the exposure time was several min. A half-wave plate was employed to control the direction of the beam polarization parallel (TE-pol) or perpendicular (TM-pol) to the fringe direction of the interference pattern. The formation of the embedded Bragg gratings was observed by the optical microscope images (1500-times magnification) as shown in Fig. 4, where the linear fringes represent the intensity distribution of the scattered light from the silver particles. The white bar in the figure represents a scale of 10 μm. The size and the volume fraction of the silver particles in the bright regions are not clearly seen by the microscope, but the volume fraction and size of the silver particles in the bright regions would be relatively larger than those in the dark. In the case of the femtosecond photoreduction[11], the silver particles protruding through the sample surface were about 100 μm in diameter. Thus we can assume that the size of the silver particles shown in the bright regions is of order of 100 mm, such that it enables for us to measure the scattered light by microscope. Before the optical microscope images an object plane at the depth of 60 mm from the glass surface, such a fringe of the scattered light distribution was not measured. Only at the depth between 60 mm to 75 μm from the surface we were able to observe the linear fringes. This 15-μm-thick grating embedded in the glass medium was also confirmed by observing the

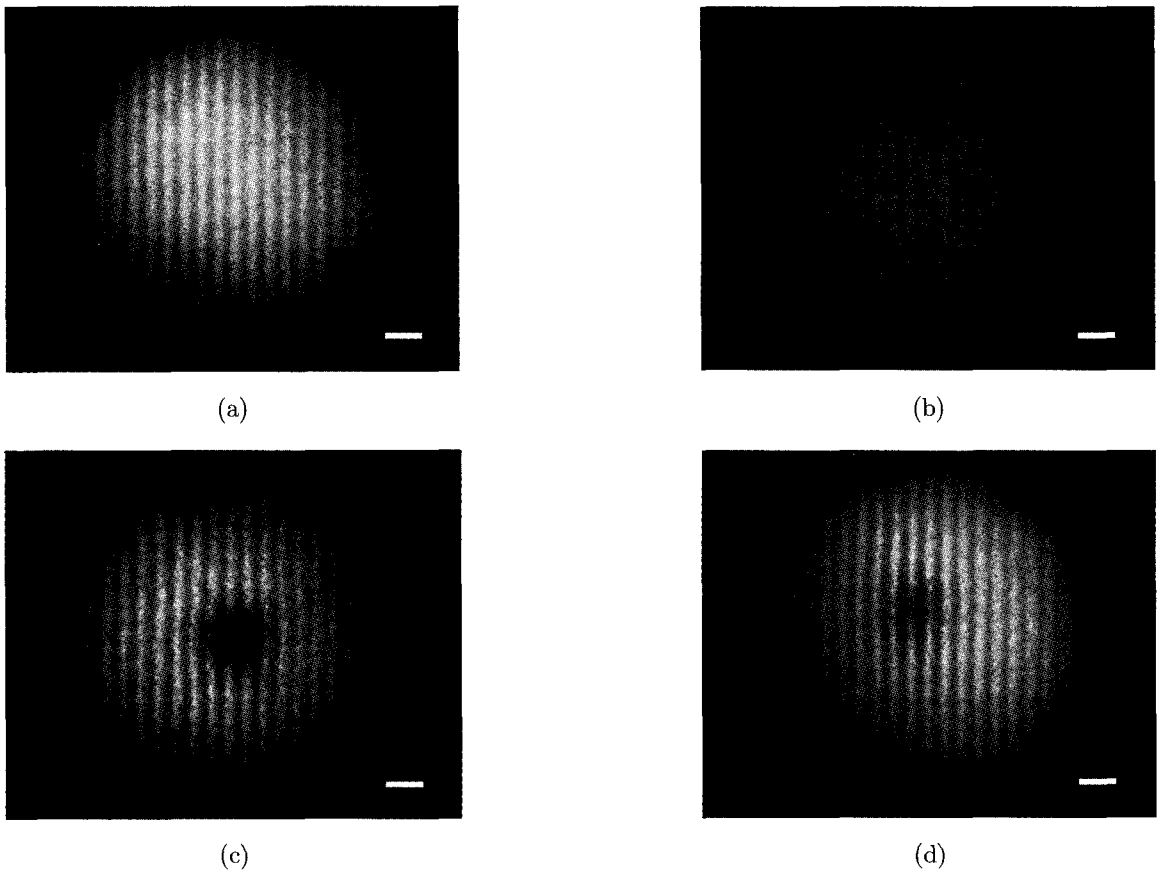

FIG. 4. Optical microscope images of the Bragg gratings created by (a) the two TE-pol beams and (b) the two TM-pol beams. And images of the Bragg gratings, which was initially created by the two TE-pol beams, after exposure by (a) a TE-pol beam and (b) a TM-pol beam at the central regions. The white bar represents 10 μm.

top surface of the glass substrate sequentially after mechanical grinding from the top surface in 1-μm steps. We found from this sequential observation that the silver particles shown in the bright fringes were continuously distributed along with the bright-fringe planes in depth direction. Therefore, we can imagine the Bragg grating as a periodic structure constructed by side-by-side setting a 1.75-μm-thick, 15-μm-wide, flat layer of silver-nanoclusters on edge with a period of 3.5 μm inside a glass substrate.

The visibility of the grating fringes shown in Fig. 4 (a), which was generated by interfering the two TE-pol beams, is much better than that by interfering the two TM-pol beams in Fig. 4 (b). The beam intensity of the exposure light and the exposure time were identical in both cases of the images. But, there was a big difference in behavior of the diffraction signal from the two kinds of gratings. For the TE-pol beams with the intensity of 10W/mm^2, the diffraction signal with a wavelength of 633 nm became to appear after 1 min illumination and there was no further change in the intensity of the diffraction signal after 4 min. The final diffraction efficiency of the grating formed by the TE-beam interference was measured as 85% in maximum. For the TM-polarized beams with the same intensity, on the other hand, it took about 8 min to reach maximum diffraction efficiency of 28%. One may consider that this dependence of the diffraction efficiency on the polarization direction could be caused by difference in the original visibilities of the interference patterns generated from the TE- and TM-beam couplings. But, the discrepancy of the two original visibilities is less than 1% since the interference angle of the two beams is about 3 degrees in the experiment.

III. DISCUSSION

It is noted that there were no further change in the diffraction efficiency of the Bragg gratings after post-annealing at 700℃ for more than 30 min. This means that the silver nanoparticles composing the Bragg gratings are very stable in its size and volume fraction to the thermal excitation. Most of the metallic nanoparticle gratings reported so far with clustering mechanisms of the ultrashort photoreduction [11,15] and the PTR (photothermorefractive) process [16], on the contrary, are not so stable that the nanoparticles disappeare after post-annealing even at 300℃. Therefore, we expect that the mechanism to form our metallic Bragg gratings would be something different from the reported ones. With only the experimental results shown in Fig. 4 (a) and (b), it is not yet enough to understand the physical reasons how the thermally stable silver-particles with the size of about 20 nm before the light exposure are arranged periodically with a size large enough to be seen by the optical microscope, and why the grating formation is influenced by the polarization direction of the interference beams. Also, it is not clear whether the bright regions with the silver clusters in the grating image correspond to the constructive interference fields or the destructive. In order to investigate those physical reasons, we conducted another experiment with a single laser-beam by focusing it onto the embedded grating layer. The exposure energy of the single beam is nearly the same as the energy used to form the Bragg grating, but the spot size at the focus is about 10 μm in diameter which is much smaller than the grating area of 200 μm. We considered again two orthogonal directions of polarization for the single exposure beam: parallel polarization (TE-pol), wherein the electric field is parallel to the grating fringe directions, and perpendicular polarization (TM-pol). Figure 4 (c) and 4 (d) show the optical microscope images after the TE-pol and TM-pol exposures, respectively. In both of the images the bright fringes near the center are diminished obviously. It means that a remarkable reduction of the density and size of the silver nanoparticles occurred during the exposures. For the TE-pol exposure shown in Fig. 4 (c), the two bright fringes at the center were almost disconnected through the whole 15-μm-depth grating planes, while there were no complete disconnections in all the fringes for the TM-pol exposure. Therefore, we can conclude that during the single-beam exposure the silver particles are reduced in its size and density gradually via photoionization of the silver metals, and that the photoionization process strongly depends on relative direction of the beam polarization to the grating fringes. Strength of the electric field around the particle is enhanced by the surface plasmon resonance, resulting in ionization of the silver metals. The silver ions are then diffused out and some of them could stick to the neighboring silver particles. Thermal excitation during the exposure must accelerate the diffusion, but it is not critical at least for the initial photoionization since the gratings were not eliminated by the annealing process at 700℃. The physical reasons for the periodic arrangement of the silver nanoparticles, as shown in Fig. 4, can be understood by these physical excitations of the particle plasmons and the thermal energy: the dark regions in the grating images, which possess fewer silver particles, correspond to the constructed fringes in the two-beam interference; the bright regions correspond to the destructive interference where aggregation of the diffused silver ions into the larger particles take places.

The strong dependence of formation and elimination of the grating on the beam polarization would be explained by the coupling effect of the neighboring particle plasmons. It is known that, even if the shape of metal particles is spherical, the excited plasmon fields are not symmetrically distributed around the

metal spheres but elliptically elongated toward the polarization direction of the incident beam [17]. The elongated plasmon fields are then coupled to each other more efficiently along with the parallel direction to the polarization than the perpendicular direction [4], and that this plasmon coupling induces red-shift for the absorption peak of the metal nanoparticles [18-20]. During the grating formation in our experiment, interference of the two TE-pol beams leads to the linear fringes with direction parallel to the beam polarization. Therefore, the electric field of the TE-polarized beams oscillates in parallel to the constructive interference fringes, resulting in the strong near-field coupling of the particle plasmons through the bright interference fringes. This coupling effect may make shift of the plasmon peaks from about the 420 nm as shown in Fig. 2 (c) toward a wavelength near the 488 nm of the exposure beams, in consequence, the coupled plasmons could be enhanced strongly enough to induce the photoionization for most of the silver particles in the bright fringes. Therefore, the TE-pol beams would be able to produce the Bragg grating with a clear periodic-distribution of the silver particles as shown in Fig. 4 (a), and the TM-pol beams produce only a poor distribution as shown in Fig. 4 (b). This plasmon coupling effect appears during the single beam exposure for erasing the gratings shown in Fig. 4 (c) and (d). The single TE-pol beam with an intense electric field oscillating along the grating fringe direction reduces the volume fraction of the silver particles dramatically, as shown in Fig. 4 (c), via photoionization activated by the strong plasmon coupling. Surface plasmon coupling between the metal particles is visualized with the FDTD (Finite Difference Time Domain) method. Figure 5 shows intensity plots of the electrical fields around the silver particle array (a) before and (b) after the light propagates through the particle array. Size of the silver particles is 20nm and the spacing between the particles is 50nm. The pulse width is $4.6\text{x}10^{-17}$ sec and the surrounding medium is air. After passing the optical pulse over the array, the particle plasmons resonantly excited at the particle surfaces are still strongly coupled to each other in the gaps between the particles.

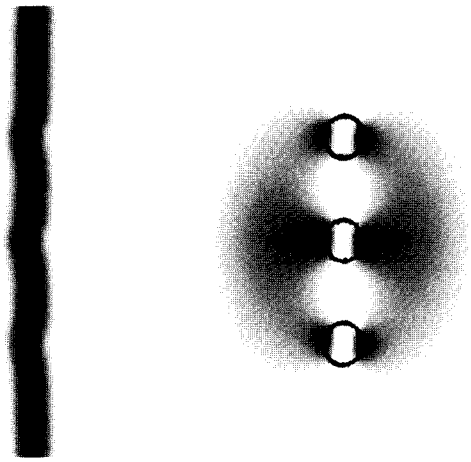

(a) (b)

FIG. 5. Intensity plots of the electrical field near the silver nanoparticle array. The calculation was done by the FDTD method. (a); during the incident light passing through the nanoparticle array, (b) 0.38 fs after the light passing through the array. Size of the silver particles is 20 nm and the spacing between the particles is 50 nm.

IV. CONCLUSION

We have found that the near-field coupling effect of the particle plasmons could be strong enough to arrange periodically the volume fraction of few tens-nm-size silver nanoparticles, and that the coupling strength strongly depends on the polarization direction of the incident beams. We have proposed a physical mechanism that the near-field coupling causes photoionization of the silver particles, leading to diffusion and aggregation to increase the volume fraction in a periodic structure. As an example of the periodic structures we have formed the metallic Bragg gratings embedded deep inside the glass medium, which are very stable to the thermal post-annealing with a constant diffraction efficiency of 85% at 633 nm. The method presented here to form an embedded Bragg grating composed of metallic nanoparticles can be utilized for realization of an arbitrary periodic distribution of metal particles in a dielectric medium and for design of novel metamaterials with a permittivity which is periodically distributed and widely dispersed in a range from negative to positive.

*Corresponding author : shsong@hanyang.ac.kr

REFERENCES

[1] U. Kreibig and M. Vollmer, *Optical Properties of Metal Clusters*, (Springer-Verlag, Heidelberg, Germany, 1995), pp. 13-123.

[2] B. Lamprecht, G. Schider, R. T. Lechner, H. Ditlbacher, J.R. Krenn, A. Leitner, and F. R. Aussenegg, "Metl Nannoparticle gratings: Influence of Dipolar Particle Interaction on the Plasmon Resonance," *Phys. Rev. Lett.*, vol. 84, no. 20, pp. 4721-4724, 2000.

[3] Stefan A. Maier, Mark L. Brngersma, Pieter G. Kik, and Harry A. Atwater, "Observation of near-field coupling in metal nanoparticle chains using far-field polarization spectroscopy," *Phys. Rev. B*, vol. 65, no. 19, pp. 1934081-1934084, 2002.

[4] M. Quinten, A. Leitner, J. R. Krenn, and F. R. Aussenegg, "Electromagnetic energy transport via linear

chains of silver nanoparticles," *Opt. Lett.*, vol. 23, no. 17, pp. 1331-1333, 1998.

[5] T. W. Ebbesen, H. J. Lezec, H. F. Ghaemi, T. Thio., and P. A. Wolff., "Extraordinary optical transmission through sub-wavelength hole arrays," *Nature*, vol. 391, no. 6668, pp. 667-669, 1998.

[6] H. J. Lezec, A. Degiron, E. Devaux, R. A. Linke,L. Martin-Moreno, F. J. Garcia-Vidal, and T. W. Ebbesen, "Beaming Light from a Subwavelength Aperture," *Science*, vol. 297, no. 5582, pp. 820-822, 2002.

[7] M.Yano, M. Fukui, M. Haraguchi, and Y. Shintani, "Insitu and real-time observation of optical constants of metal films during growth," *Surf. Sci.*, vol. 227, no., pp. 129-137, 1990.

[8] N. Garcia, E. V. Ponizovskaya, and J. Q. Xiao, "Zero permittivity materials: Band gaps at the visible," *Appl. Phys. Lett.*, vol. 80, no. 7, pp. 1120-1122, 2002.

[9] J. Yoon, G. Lee, S. H. Song, C. Oh, and P. Kim, "Surface-plasmon photonics band gaps in dielectric gratings on flat metal surface," *J. Appl. Phys.*, vol. 94, no. 1, pp. 123-129, 2003.

[10] S. Foteinopoulou, E. N. Economou, and C. M. Soukoulis, "Refraction in media with a negative refractive index," *Phys. Rev. Lett.*, vol. 90, no. 10, pp. 1074021-1074024, 2003.

[11] Koshiro Kaneko and Hong-Bo Sun, Xuan-Ming Duan, Satoshi Kawata, "Two-photon photoreduction of metallic nanoparticle gratings in a polymer matrix," *Appl. Phys. Lett.*, vol. 83, no. 7, pp. 1426-1428, 2003.

[12] M. Kaempfe, T. Rainer, K.-J. Berg, G. Seifert, and H. Graener, "Ultrashort laser pulse induced deformation of silver nanoparticles in glass," *Appl. Phys. Lett.*, vol. 74, no. 9, pp. 1200-1202, 1999.

[13] S.Slraj Najafi, *Introduction to Glass Integrated Optics*, (Artech House, Boston, USA, 1992), pp. 7-38.

[14] I. Tanahashi, M. Yoshida, Y. Manabe, and T. Tohda, "Effects of heat treatment on Ag particle growth and optical properties in Ag/SiO_2 glass composite thin films," *J. Mater. Res.*, vol. 10, no. 2, pp. 362-365, 1995.

[15] C.montero, C. Gomez-Reino, and J. L. Brebner, "Planar bragg gratings made by excimer-laser modification of ion-exchanged waveguides," *Opt. Lett.*, vol. 24, no. 21, pp. 1487-1489, 1999.

[16] O. M. Efimov, L.B. Glebov, L. N. Glebova, K. C. Richardson, and V. I. Smirnov, "High-efficiency bragg gratings in photothermorefractive glass," *Appl. Opt.*, vol. 38, no. 4, pp. 619-627, 1999.

[17] Daniel L. Feldheim and Colby A. Foss, Jr., *Metal Nanoparticles*, (Marcel Dekker, New York, USA, 2002), pp. 110-113.

[18] Hiroharu Tamarua, Hitoshi Kuwata, Hideki T. Miyazaki, and Kenjiro Miyano, "Resonant light scattering from individual Ag nanoparticles and particle pairs," *Appl. Phys. Lett.*, vol. 80, no. 10, pp. 1826-1828, 2002.

[19] W. Rechberger, A. Hohenau, A. Leitner, J.R. Krenn, B. Lamprecht, and F.R. Aussenegg, "Optical properties of two interacting gold nanoparticles," *Opt. Commun.*, vol. 220, no. 1-3, pp. 137-141, 2003.

[20] Zhengxin Liu, Honghong Wang, Hao Li, and Xuemei Wang, "Red shift of plasmon resonance frequency due to interacting Ag nanoparticles embedded in single crystal SiO_2 by implantation," *Appl. Phys. Lett.*, vol. 72, no. 15, pp. 1823-1825, 1998.